Received 00th January 20xx,
Accepted 00th January 20xx

DOI: 10.1039/x0xx00000x

www.rsc.org/

Healing damaged coatings using friction-sensitive hybrid microcapsules

Sonia García-Jimeno,[a] Mary Cano-Sarabia,*[a] Nereida Mejias,[a] Virtudes Navarro,[b] Ana Belen Frances,[b] and Daniel Maspoch*[ac]

[a.] *Institut Catala de Nanociencia i Nanotecnologia, Esfera UAB, 08193, Bellaterra, Spain*

[b.] *Centro Tecnológico del Mueble y la Madera de la Región de Murcia (CETEM), 30510, Yecla, Spain.*

[c.] *Institució Catalana de Recerca i Estudis Avançats (ICREA), 08100, Barcelona, Spain*

† Electronic Supplementary Information (ESI) available: Experimental details, characterization and additional Scratch-and-Repair images. See DOI: 10.1039/x0xx00000x

A new healing surface coating technology based on incorporation of hybrid melamine-formaldehyde-polyurethane (MF/PU) microcapsules which contain a healing mixture, into standard polyurethane surface coatings, is described. Microcapsules release the healing mixture upon surface scratching after a mechanical damage.

Microcapsules are among the most attractive materials currently available for use in consumer products, as they can easily be tuned for myriad functions[1] such as protection (of sensitive components), masking (of organoleptic properties), isolation (of toxic materials) and controlled targeted release (of an active encapsulated substance). An illustrative example is the Scratch-and-Sniff capsules containing perfumes, which are now incorporated in most of the softeners found in the supermarkets for providing long-lasting fragrance in dried clothes. Herein, we described a microcapsule-based technology for Scratch-and-Repair healing of surfaces under ambient conditions. In it, microcapsules containing a stable liquid healing mixture are incorporated into a standard polyurethane wood varnish. In the resulting functionalized coating, surface healing occurs in two steps: firstly, cracks in the coating surface liberate the embedded capsules into the surrounding area, such that they end up mainly in the created burrs; and secondly, scratching of the damaged area (e.g. with a furniture cloth) simultaneously breaks and drives the microcapsule contents into the cracks for repair. Specifically, the released healing agent acts as an internal glue by bonding the crack faces. It quickly hardens upon exposure to air via solvent evaporation, without any need for catalysts or external heat sources. In fracture experiments performed on a damaged model wood surface, we observed 90% recovery in polymer coating toughness and 80% filling of crack depth.

Most materials, such as the metals or wood typically used to fabricate railings and furniture, are susceptible to damage due to superficial cracks, which are very difficult to repair. Cracking in the surface coating leaves the underlying material exposed to harmful elements (e.g. humidity, cleaning products, sea water, etc.).[2] One obvious solution to this problem is to develop self-healing polymeric coatings. To date, numerous strategies that have been proposed to this end, most of which entail the use of self-healing polymers and/or the use of microcapsules.[2-7] One example is thermo-responsive self-healing polyurethanes with shape memory, which are based on Diels-Alder reaction between furan and maleimide moieties.[5] Another example is incorporation of a microencapsulated liquid monomer into a polymer coating containing a dispersed catalyst:[2,5,8] fracture of the polymer coating breaks the microcapsules, consequently releasing the monomer, which in turn reacts with the catalyst to repair the fracture. Another reported approach is the use of nanoparticle-filled oil droplets that can find cracks on a surface and temporarily adhere to crack interiors, where they selectively deliver the nanoparticles for repair.[9] More recently, self-healing coatings based on microencapsulation of solvents (e.g. xylene, hexane or chlorobenzene),[10] epoxy resin,[11] isocyanates[12,13] or oils (e.g. linseed and tung)[14-17] have been reported.

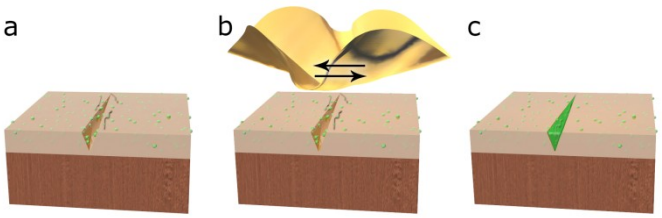

Fig. 1 Overview of Scratch-and-Repair concept. A microencapsulated healing agent is embedded in a standard polyurethane coating such as common wood varnish (from left to right): (a) Surface damage generates a crack, moving the polyurethane coating and the microcapsules around to form burrs. (b) Scratching of the damaged area with a cloth breaks the microcapsules, which release the healing mixture into the crack, where it hardens upon exposure to air. (c) The resulting self-repaired surface.

To validate our proposed technology, we selected the case of a standard polyurethane-based wood varnish. Figure 1 illustrates the Scratch-and-Repair process: firstly, the microcapsules are liberated upon fracture of the varnish coating; secondly, scratching of the damaged area with a simple cloth simultaneously moves the microcapsules to the crack faces and breaks them, releasing their liquid healing mixture into the cracks, where it hardens (via solvent evaporation upon exposure to air) to seal the crack. The microcapsules were designed according to several requirements.

Initially, we designed the contents of the microcapsules to do the following: to be compatible with the polyurethane-based varnish; to be stable and to not solidify while inside of the microcapsules; to be sufficiently mobile to flow into the cracks upon release; and to dry, solidify and seal the crack simply upon contact with the air, without the need for any catalyst or external heating.[18] We selected a mixture of a blocked polyisocyanate built from isophorone diisocyanate (IPDI; Desmodur® PL 340 BA/SN; Bayer) units (also containing 60% [w/w] of butyl acetate and naphtha solvent at a ratio of 18:22)[12] and the castor oil at a ratio of 4:1. We chose castor oil because it increases the pot life of isocyanates in solution[19] and it ameliorates the fluidity ($viscosity_{IPDI+castor\ oil}$ = 420 mPa·s vs. $viscosity_{IPDI}$ = 600 mPa·s) of the healing mixture. Moreover, it acts as an internal plasticizer, such that, when the solvents of the mixture evaporate in air, the contents solidify into a solid film whose indentation hardness is similar to that of the varnish (*vide infra*).

We tuned the microcapsule wall to be sufficiently resistant to spraying and to crack formation, but still labile to scratching. Importantly, our initial experiments with pure melamine-formaldehyde (MF) or polyurethane (PU) microcapsules were unsuccessful: the former broke during spraying, whereas the latter did not break during scratching (vide infra). Thus, we reasoned that MF/PU hybrid microcapsules[20-22] would offer the best balance, so we fabricated a batch via interfacial polymerization. Specifically, we prepared an oil-in-water emulsion, in which the water phase contained polyEMA (3.3%), melamine-formaldehyde (MF; Beetle® PT312; BIP Limited) pre-polymer and sodium hydroxide (1.3% wt), and the oil ("core") phase contained hexamethylene diisocyanate (HDI; Bayhydur® XP 2547; Bayer), castor oil and IPDI. Then, the pH of the emulsion was adjusted to 5 using formic acid and the temperature of the reaction was raised to 65 ºC under stirring. After 3 hours, the resulting MF/PU microcapsules were cleaned with a mixture of methanol/water, resuspended in acidic water (pH = 5), and finally, the resultant suspension was spray-dried at 130 ºC to afford a fine white powder (encapsulation yield = XX %).[23]

Scanning Electron Microscopy (SEM) images of the aforementioned powder revealed spherical microcapsules (diameter: 13 ± 4 μm) (Figure 2a). The average size of these microcapsules was subsequently confirmed by laser diffraction

measurements (Figure S2). The synthesized capsules were also characterized by embedding them in a polymeric EPON resin, cutting this resin into nanometric slices (average thickness: 120 nm) using a microtome, and then analyzing the slices by High-Resolution SEM. The images acquired with the in-lens secondary electron (SE) detector and the energy selective backscattered (EBS) detector confirmed the core-shell structure of the MF/PU microcapsules, whose shell was formed by a single wall (thickness: *ca.* 330 ± 80 nm) (**Figure 2c**). Notably, formation of a uniform single-wall shell is not typical for hybrid microcapsules, as previously reported hybrid MF/PU capsules contained either a double-shell[24,25] or granulated single-walls. The single-wall was further confirmed by elemental mapping with energy dispersive X-ray spectrometry (EDX) on a single core-shell structure, which revealed a highly uniform distribution of N atoms in the shell (Figures 2d and S3). Additionally, solid-state ^{13}C NMR confirmed the hybrid MF/PU composition of the single-wall shell: the spectrum revealed two characteristic signals (Figure S4): one at 158 ppm, which corresponds to the carbonyl groups of the urea bonds formed upon reaction of the isocyanates of HDI with the secondary amines from the MF resin; and one at 183 ppm, which corresponds to the shift of the aromatic carbons of melamine following said reaction. In addition, the spectrum completely lacked the signal (at 122 ppm) corresponding to the isocyanate groups of HDI.

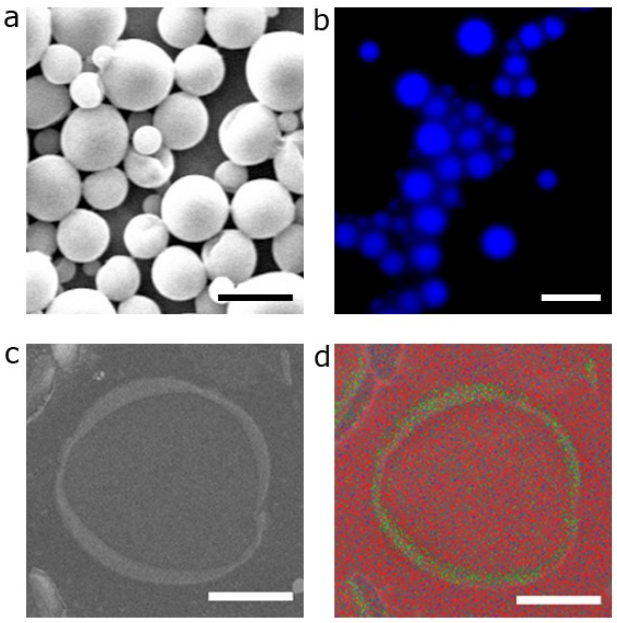

Fig. 2 Microcapsule characterization. (a) Representative SEM image of the synthetized spherical MF/PU microcapsules. (b) Fluorescent optical microscopy image of the MF/PU microcapsules labeled with pyrene. (c,d) Backscattered SEM image of a microtome section of a microcapsule wall and corresponding element map for N (green) and C (red), using low voltage EDS (2KV). Scale bars: 20 µm (a,b) and 5 µm (c,d).

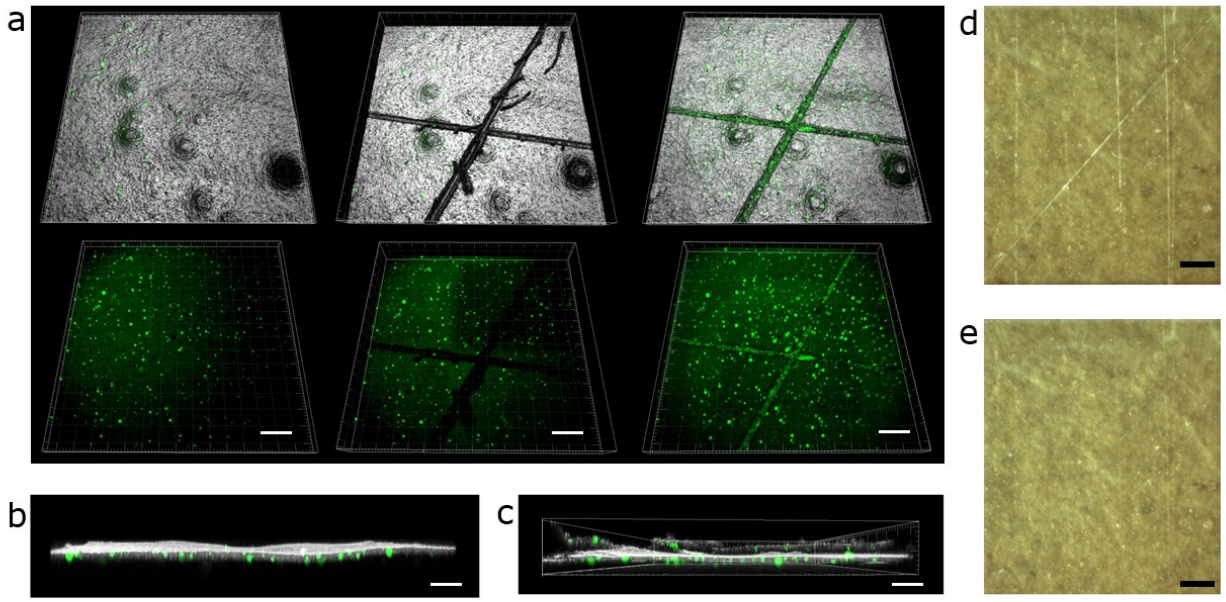

Fig. 3 *Scratch-and-Repair* experiment on wood surfaces. (a) CLSM images (top: reflection; bottom: transmitted) of fluorescently labeled microcapsules dispersed in a polyurethane matrix (left); and of the surface after being damaged with a scalpel (center) and after subsequent scratching of the damaged area (right). (b,c) CLSM images (side-view) of the polyurethane matrix with embedded microcapsules before (b) and after (c) the surface damage (right), revealing the microcapsules at the crack burrs. (d,e) Optical images of the wood surface after the mechanical damage (d) and following the Scratch-and-Repair experiment (e). Scale bars: 200 µm (a), 100 µm (b,c) and 1 mm (d,e).

Optimizing the micromechanical properties of the microcapsules was essential for ensuring that the healing surface coating technology performed correctly: the microcapsules had to remain intact during spray-drying and crack formation, yet had to break upon scratching of the surface. Thus, we studied the micromechanical strength of the hybrid MF/PU microcapsules and of their corresponding pure MF or PU analogs (fabricated in similar sizes and under identical synthetic conditions) by nanoindentation. Encouragingly, the rupture force of the MF/PU microcapsules (0.75 mN; Figure S5) was greater than that of the pure MF microcapsules (0.22 mN), which fractured during spray-drying (Figure S6a-c), but far smaller than that of the PU microcapsules (15.52 mN), which did not break when the surface is subjected to scratching (Figure S6e-f).

Since the healing mixture (IPDI/castor oil) inside the microcapsules had to remain liquid until released to the air, we sought to confirm the temporal stability of the encapsulated core mixture. Thus, we compared the micromechanical properties of fresh MF/PU microcapsules to those of MF/PU microcapsules that had been stored for 4 months at room temperature. Importantly, we found that storage did not affect either the rupture force (0.75 mN) or the Young's modulus (2.03 GPa) of the microparticles; thus, we concluded that the healing mixture had remained liquid. Interestingly, the presence of castor oil in the core mixture proved to be crucial for this stability: the rupture force of MF/PU microcapsules containing only IPDI increased over time, from 1.34 mN (fresh) to 3.46 mN (after 4 months storage), suggesting gradual solidification of the IPDI core.

To experimentally track the Scratch-and-Repair effect, we prepared fluorescently labeled MF/PU microcapsules in which we added the fluorescent label pyrene (0.12% w/w) to the healing

mixture (IPDI/castor oil) (Figure 2b). Dried microcapsules (10% w/w) were then dispersed in a 2K polyurethane matrix under stirring, and the resulting mixture was sprayed over a wood surface using a compressed air gun. This substrate was finally dried at room temperature for 48 hours to form a varnish coating (thickness: 100 ± 5 µm; rugosity: 5 ± 1.5 µm) (Figure S7) in which the microcapsules were uniformly distributed (Figure 3a). We mechanically damaged this substrate with a scalpel to induce perpendicular cracking of the varnish coating, and then monitored the healing surface coating effect by confocal laser scanning microscopy (CLSM) (see Figures 3a and S8). Confocal profilometry characterization of the damaged substrate revealed cracks with widths of ~49 µm and depths of ~27 µm (Figure 4b). Close inspection of the damaged surface by CLSM and FE-SEM revealed that, when a crack had formed, the polyurethane-based varnish was removed together with the microcapsules, forming burrs at the edges of the cracks in which the microcapsules localized (Figures 3b,c and S9). These images clear indicated that the microcapsules remain intact during crack formation and that repair occurs upon scratching of the damaged area (e.g. with a furniture cloth or a finger). Figure 3c-e and Video S1 show the results of the Scratch-and-Repair experiment, in, which the cracks disappear upon repair. Figure 3c reveals the preferential depositing of the healing agent into the crack: note that the fluorescence emanates predominately from the cracked region. We then studied the degree of crack repair by confocal profilometry. Figure 4b shows that the filled cracks exhibited a depth of ~ 4 µm, which translates to a recovery of ~ 90 % of the original fracture depths. We then performed a similar experiment on a varnish coating without microcapsules. As expected, we did not observe any repair of the damaged area (Figures S10). We reasoned that the friction generated during scratching enables accessible microcapsules (released during crack formation and localized mainly at the burrs) to be transported preferentially to and broken in the cracks, where they release the healing mixture. Further evidence of the movement of the microcapsules was provided by the SEM images of the same region of a burr before and after the scratch: none of the localized microcapsules that appeared in the former were present in the latter.

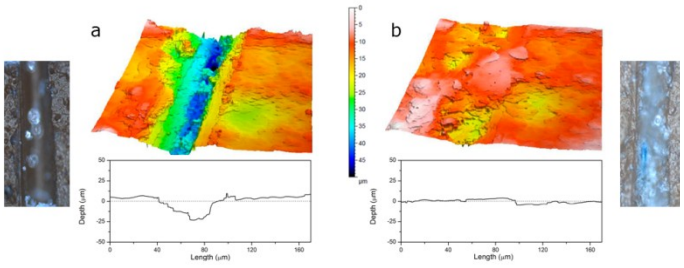

Fig. 4 3D confocal profilometry images (surface topography), roughness profiles (along a diagonal) and optical microscopy images of the test wood surface in a Scratch-and-Repair experiment before (a) and after (b) repair.

Completion of the healing process requires solidification of the healing mixture in the crack. We gathered evidence for solidification of the healing mixture by studying the repaired crack directly by nanoindentation. As expected, the hardness (0.04 ± 0.01 GPa) and Young's modulus (2.20 ± 0.64 GPa) of the repaired areas were comparable to the hardness (0.06 ± 0.02 GPa) and Young's modulus (2.24 ± 0.67 GPa), respectively, of the undamaged areas. These findings are consistent with the fact that the healing mixture has a similar composition to that of the surrounding matrix, such that repair maintains structural homogeneity and uniformity in the surface.[27] We then studied solidification of the healing mixture upon exposure of it to air, and found that it is governed chiefly by a physical phenomenon driven by the solvent evaporation (butyl acetate and naphtha) as confirmed by ^{13}C-NMR, MALDI-TOF and FTIR (Figures S11-S13). This process leads to hard film formation that results from the associative interactions between the molecular chains.[19]

Having determined that hardening of the healing mixture does not involve polymerization, we next investigated the stability of the solidified healing agent in the crack to commercial wood cleaner, water and organic solvents, including ethanol and acetone. Importantly, cleaning of the repaired zone and surrounding areas with a cloth impregnated with wood cleaner, water or ethanol did not lead to any changes in or dragging of the solidified healing agent; however, when acetone was used the healing agent was removed. Hence, to increase the stability of the repaired surface to potentially aggressive solvents, we tested incorporation of the catalyst dibutyltin dilaurate (DBTL) into the healing mixture (IPDI/castor oil) followed by heating of the resultant mixture. As revealed by a new Scratch-and-Repair experiment, the catalyst drove reaction of the unblocked isocyanate groups of the IPDI with the hydroxyl groups of the castor oil at 200 ºC,[28] forming the well-known castor oil-based polyurethane polymer,[29] as confirmed by IR (Figures S14-S16). As expected, this repaired surface was stable to acetone.

Conclusions

In summary, we have reported a new healing surface coating technology. It is based on incorporation of a new type of hybrid MF/PU microcapsules, which contain a healing mixture, into standard polyurethane surface coatings (e.g. common wood varnish). The microcapsules are sufficiently robust to be incorporated into polymeric films, yet sufficiently fragile to be cracked upon scratching, to release the healing mixture for crack repair. We are confident that our technology could be harnessed to increase the reliability and service life of the polyurethane films typically used in the furniture industry. It might also be used to protect sturdier materials, such as metals, ceramics and glasses, offering new solutions for many industrial sectors (e.g. construction) in which smarter materials with longer service lives are in demand.

Acknowledgments

We thank the MICINN (Spain) for financial support through the project INNPACTO 2011-1229-020000, and Dr. Carles Carbonell for his assistance in designing some of the graphics. ICN2 acknowledges support of the Spanish MINECO through the Severo Ochoa Centers of Excellence Program under Grant SEV-2013-0295.

References

1 F. Caruso, *Chem. Eur. J.*, 2000, **6**, 413-419.
2 S. R. White, N. R. Sottos, P. H. Geubelle, J. S. Moore, M. R. Kessler, S. R. Sriram, E. N. Brown and S. Viswanathan, *Nature*, 2001, **409**, 794-797.
3 T. Szabó, L. Molnár- Nagy, J. Bognár, L. Nyikos and J. Telegdi, *Prog.Org.Coat*., 2011, **72**, 52-57.

4 Y.-K. Song, Y.-H Jo, Y.-J. Lim, S.-Y Cho, H.-C.Yu, B.-C. Ryu, S.-I. Lee and C.-M. Chung, *ACS Appl. Mater. Interfaces*, 2013, **5**, 1378-1384.
5 Y. Yang and M. W. Urban, *Chem. Soc. Rev*., 2013, **42**, 7446-7467.
6 X. J. Ye, J.-L. Zhang, Y. Zhu, M. Z. Rong, M. Q. Zhang, Y. X. Song and H.-X. Zhang, *ACS Appl. Mater. Interfaces*, 2014, **6**, 3661-3670.
7 S. H. Cho, S. R. White, P. V. Braun, *Adv. Mater.*, 2009, **21**, 645-649.
8 M. Samadzadeh, S. H. Boura, M. Peikari, S. M. Kasiriha and, A. Ashrafi, *Prog. Org. Coat., 2010,* **68**, 159-164.
9 K. Kratz, A. Narasimhan, R. Tangirala, S. Moon, R. Revanur, S. Kundu, H. S. Kim, A.J. Crosby, T. P. Russell, T. Emrick, G. Kolmakov and A.C. Balazs, *Nat. Nanotechnol*., 2012, **7**, 87-90.
10 M. M. Caruso, D. A. Delafuente, V. Ho, N. R. Sottos, J. S. Moore and S. R. White, *Macromolecules*, 2007, **40**, 8830-8832.
11 T. Yin, L. Zhou, M. Z. Rong and M. Q. Zhang, *Smart Mater. Struct.*, 2008, **17**, 015019.
12 J. Yang, M. W. Keller, J. S. Moore, S. R. White and N. R. Sottos, *Macromolecules*, 2008, **41**, 9650-9655.
13 X. K. D. Hillewaere, R. F. A. Teixeira, L. T. T. Nguyen, J. A. Ramos, H. Rahier and F. E. Du Prez, *Adv. Funct. Mater.*, 2014, **24**, 5575-5583.
14 M. Behzadnasab, M. Esfandeh, S.M. Mirabedini, M. J. Zohuriaan-Mehr and R.R. Farnood, *Colloids Surf., A,* 2014, **457**, 16–26.
15 T. Szabó, J. Telegdi and L. Nyikos, *Prog. Org. Coat.*, 2015, **84**, 136-142.
16 P.R. Hondred, L. Salat, J. Mangler and M.R. Kessler, *J. Appl. Polym. Sci.*, 2014, **131**, 40406/1-40406/9.
17 M. M. Samadzadeh, S. H. Boura, M. Peikari, A. Ashrafi and M. Kasiriha, *Prog. Org. Coat.*, 2011, **70**, 383-387.
18 M. M. Caruso, B. J. Blaiszik, H. Jin, S. R. Schelkopf, D. S. Stradley, N. R. Sottos, S. R. White and J. S. Moore, *ACS Appl. Mater. Interfaces*, 2010, **2**, 1195-1199.
19 U. Meier-Westhues, *Polyurethanes: Coatings, Adhesives and Sealants*, Vincentz Network GmbH & Co KG, Hannover, Germany 2007, Ch. 5.
20 T. Nesterova, K. Dam-Johansen and S. Kiil, *Prog.Org.Coat*., 2011, **70**, 342-352.
21 M. Huang and J. Yang, *J. Mater. Chem*., 2011, **21**, 11123-11130.
22 J. M. Asua, *Prog. Polym. Sci.*, 2002, **27**, 1283-1346.
23 W. Mehnert and K. Mader, *Adv. Drug Deliv. Rev.*, 2001, **47**, 165-196.
24 G. Li, Y. Q, Feng, P. Gao and X. G. Li, *Polym. Bull*., 2008, **60**, 725-731.
25 D. Sun, J. An, G.Wu and J. Yang, *J. Mater. Chem*. A, 2015, **3**, 4335-4444.
26 S. Neuser, E. Manfredi and V. Michaud, *Mater. Chem. Phys*., 2014, **143**, 1018-1025.
27 E. B. Murphy and F. Wuld, *Prog. Polym. Sci*., 2010, **35**, 223-251.
28 R. Molder, F. Plogmann and P. Speier, *J. Coatings Technol.*, 1997, **69**, 51-57.
29 I. S. Ristić, J. Budinski-Simendić, I. Krakovsky, H. Valentova, R. Radićević, S. Cakić and N. Nikolić, *Mater. Chem. Phys*., 2012, **132**, 74-81.